

The triplet He_2^* Rydberg states and their interaction potentials with ground state He atoms

J. Eloranta^{a)} and V. A. Apkarian

Department of Chemistry, University of California, Irvine, California 92697-2025

(Received 24 January 2001; accepted 20 April 2001)

We report *ab initio* potential energy curves for the interaction of ground state He atoms with the triplet He_2^* excimers. Fully converged, unrestricted, open-shell, coupled-cluster method including singles, doubles, and perturbative treatment of triples substitutions (UCCSD(T)) is used to compute the He_2^* -He potential energy curves for the $a(^3\Sigma_u)$ and $c(^3\Sigma_g)$ states. The internally contracted multireference configuration interaction method (ICMRCI) is used to compute the potential energy curves for $a(^3\Sigma_u)$, $b(^3\Pi_g)$, $d(^3\Sigma_u)$, $e(^3\Pi_g)$, $f(^3\Sigma_u)$, and $f(^3\Pi_u)$ states. Where they can be compared, at the potential minima, the ICMRCI and UCCSD(T) methods agree to within 1 cm^{-1} . The method reproduces the diatomic He_2 potential with an accuracy of 0.8 cm^{-1} . An accuracy of $\sim 2\text{ cm}^{-1}$ is estimated for all reported He_2^* -He potentials. Calibrations based on Li-He and H_2 -He interactions are consistent with this expectation. Calculations on tetratomics, He- He_2^* -He, are carried out to assess the nonadditivity of potentials in various states. At short range, nonadditivity arises from polarization effects, while at long-range its nonadditivity is due to the distortion of the Rydberg electron density by the ground state He atoms. Besides potential energy points, electron density plots are provided. © 2001 American Institute of Physics. [DOI: 10.1063/1.1378325]

I. INTRODUCTION

The intrinsic electronic excitations in superfluid He, the lowest of which lies at $\approx 18\text{ eV}$ above ground state,¹ can be optically accessed using strong fields provided by femtosecond laser pulses.² The sudden access of such states allows time-resolved studies of the response of the superfluid bath to molecular scale perturbations.³ In the analysis of such experiments, it is necessary to separate energetic and dynamic contributions that control the observables. Of fundamental interest is the potential energy of interaction between an electronic excitation and the liquid, which is ultimately related to the energetics of interaction between electronically excited and ground state He atoms, which is the subject of scrutiny in this paper.

The lowest energy electronic excitations in LHe are the He_2^* diatomic Rydberg states.¹ These excimers are bound by $\approx 2\text{ eV}$ relative to the $\text{He}^* + \text{He}$ asymptote, and consist of a nested stack of singlet and triplet states in which a Rydberg electron orbits the tight He_2^+ ion core ($R_{\text{He-He}} = 1.1\text{ \AA}$).^{4,5} Based on the observation of rotational wings on selected transitions,⁶ and based on analyses of spectral shifts in absorption and emission,^{7,8} it has been recognized that the He_2^* excimers occur in bubble states in liquid He. In effect, due to the repulsive exchange energy between the closed shell He and the Rydberg electron of the excimer, the liquid is repelled from the center to form a cavity shaped by the balance of forces between Pauli repulsion and surface tension. At equilibrium, the size and shape of the bubble (the angle dependent density profile of the liquid around the excimer),

must be defined by the He_2^* -LHe interaction potential, which in turn is controlled by the He_2^* -He potential energy surface. We focus on the triplet He_2^* states, and in particular the seven lowest states— $a(^3\Sigma_u)$, $b(^3\Pi_g)$, $c(^3\Sigma_g)$, $d(^3\Sigma_u)$, $e(^3\Pi_g)$, $f(^3\Sigma_u)$, and $f(^3\Pi_u)$ —which are accessible through the strong-field preparation method,² and are potentially relevant to the time-resolved studies. We first calculate the energetics and electronic wave functions of the triplet excimers in their various states. The electronic structures of the triplet states very closely resemble those of their singlet counterparts.⁵ The latter have been calculated previously using generalized valence bond theory, and then again, the main motivation was to rationalize the bubble nature of solvation of these excimers in LHe. We then compute the electronic structure of the triatomic excited states, namely, He_2^* -He, states in which the tightly bound excimer weakly interacts with a ground state He atom. We obtain the weak He_2^* -He interaction potentials by converged, high-level, *ab initio* methods. To establish that the desired accuracy is attained, we use several points of reference. The energetics of the diatomics, both ground state He-He and excited state He^* -He known from experiment and theory, provides one source for calibration. Additionally, we consider the closely related systems of Li-He and H_2 -He. Beside the accuracy of the triatomic interaction potential, to proceed from He_2^* -He to the description of He_2^* - He_n an assessment of the nonadditivity of interactions is quite crucial. The description of collective interactions and bubble structures will be taken in detail in the follow-up paper.⁹ Here, we investigate the magnitude of many-body contributions by explicitly computing and comparing the energetics of the triatomic He_2^* -He and tetrameric He- He_2^* -He in various states and geometries.

^{a)}Permanent address: Department of Chemistry, University of Jyväskylä, P.O. Box 35, FIN-40351, Jyväskylä, Finland.

II. METHODS

The interaction of the first excited triplet state of atomic helium, He^{*}(³S), with a ground state He atom, leads to the formation of the two lowest, triplet Σ excited states of He₂, namely, the *a*(³Σ_u) and *c*(³Σ_g) states with electron configurations 1σ_g²1σ_u2σ_g and 1σ_g²1σ_u2σ_u at equilibrium. By choosing suitable configurations, these states can be made the lowest energy state of their respective symmetry, and as such their energetics and interactions with ground state He(¹S) atoms could be calculated by the unrestricted open shell coupled cluster method including singles, doubles, and perturbative treatment of triples substitutions (UCCSD(T)).¹⁰ The reference state was obtained from prior open shell restricted Hartree–Fock (RHF) calculations. The spin adaptation problem in the UCCSD(T) calculations was controlled by observing the expectation values of the $S^2 - S_Z^2 - S_Z$ operator, which essentially gives deviation of S^2 from the requested spin value, and by performing restricted CCSD(T) (RCCSD(T)) (Ref. 11) calculations on selected systems. The expectation value of $S^2 - S_Z^2 - S_Z$ was always below 0.0007. To verify that the single HF reference state used in these CC calculations is adequate, we monitor the norm of the T_1 vector (amplitudes of the single excitations). It has been suggested that norm values below 0.02 indicate that the contribution of single excitations is small and thus a single reference state is sufficient.¹² The T_1 diagnostic test was fulfilled except on the steep repulsive wall of the He₂^{*}–He potential. This implies that at long distances, in the di- and triatomic ICMRCI calculations that will be described below, the multireference space merely provides a proper simultaneous convergence to all the desired excited states of the He₂^{*} and provides some important additional excitations to account for electron correlation. The calculated diatomic (³*a*, ³*c*) potential curves agree within the reported accuracy with those determined experimentally through differential scattering measurements and calculations.¹³ At the present level of theory, the He₂ ground state interaction energy is 0.85 meV and its equilibrium distance is 3.0 Å, to be compared with what is regarded as the best determination of 2.964 Å and 0.95 meV.¹⁴ Despite the very weak nature of these interactions, the good agreement is not entirely surprising. It has previously been demonstrated, in calculations of rare gas interactions including He₂, that converged coupled clusters calculations yield highly accurate potentials for weak, nonbonded interactions.¹⁵

The CCSD(T) method is only applicable for the lowest state of a given symmetry. Therefore, a point group should be chosen for the triatomic system such that each excited Rydberg state in question maps into a unique symmetry representation. This requirement cannot be fulfilled for the linear He₂^{*}–He configuration where both ³*a* and ³*c* curves correlate with A_1 representation of C_{2v} . In this case, by including a fourth ground state He atom, and demanding that the bond lengths for both ground state He atoms are equal, the symmetry can be raised from C_{2v} to D_{2h} , where the ³*a* and ³*c* states are given by the B_{1u} and A_g representations. If many-body effects are negligible, then under the assumption of additivity, this symmetry extension can approximate the

interaction energy of the triatomic. The main purpose of the present CCSD(T) calculations is to obtain accurate basis set superposition error (BSSE) corrected potentials for ³*a* and ³*c* states interacting with the ground state He atom.

Because of the symmetry imposed limitations involved with the CCSD(T) method, another approach must be taken for the higher states. Internally contracted multireference configuration interaction method (ICMRCI) (Ref. 16) with state averaged multiconfiguration self-consistent field (MC-SCF) reference calculation,¹⁷ employing complete active space (CAS) orbitals, is a general and effective method for obtaining such states. Di- and tetra-atomic calculations were performed within D_{2h} symmetry whereas for triatomic calculations C_{2v} was used. For calculation of the diatomic PES the orbitals required for describing correct dissociation were included in the CAS. For tri- and tetra-atomic calculations, when the excimer center was held fixed at the equilibrium ($R_e = 1.05$ Å), only the required lowest energy excimer molecular orbitals were included in the CAS. All obtained energies are subject to the multi-reference analogue of the Davidson correction in order to obtain approximate size-consistency.¹⁸ Rydberg orbitals were obtained from the ICMRCI calculation by performing natural orbital analysis with contour plotting provided by the MOLDEN program.¹⁹ In each case, the Rydberg natural orbital occupation number was close to unity and no ambiguity in assignment arises. For calculation of transition moments a single point calculation with all the previously mentioned orbitals in the CAS was performed (a total of 11 states averaged with identical weights). Using these reference configurations the electric dipole transition moments between the relevant states were calculated by using the wave functions obtained from ICMRCI calculations. Degeneracy of states for Σ ↔ Π transitions is accounted for by multiplying the transition moment by 2.

To obtain accurate results for interaction energies, the high quality basis set of Dunning *et al.*²⁰ (aug-cc-pV5Z; av5z), (aug-cc-pV6Z; av6z) and the specially tailored He basis sets,²¹ were used. The av5z and av6z bases have been constructed for ground state He atoms, but they contain sufficiently diffuse Gaussians to allow proper description of some of the Rydberg states. For example, with the full configuration interaction (FCI)/av5z calculation the atomic He 1s ↔ 2s transition lies at 19.87 eV, which is in good agreement with the experimental value of 19.82 eV. However, the 1s ↔ 2p transition is already off by more than 1 eV. The basis set of Ref. 21, which has been prepared for calculation of the He₂ excimers, provides correct atomic asymptotic behavior for 1s, 2s, 2p, 3s, and 3p shells. This basis set has considerably fewer Gaussians devoted for describing electron correlation, and as such, required testing to determine the severity of this deficiency.

Given the small interaction energies at issue, removal of BSSE is crucial. This was accomplished by the approximate counterpoise procedure of Boys and Bernardi.²² In the present case the correction is made by the following relation:

$$E(R) = E(R_{\text{He-He}_2^*}) - E(R_{D_u\text{-He}_2^*}) - E(R_{\text{He-}D_u^*}), \quad (1)$$

where D_u represents an atomic center with all basis functions but no charge or electrons. In all calculations the He₂^{*} bond

length was fixed at 1.05 Å. Diatomic calculations were not subject to the BSSE correction except for the singlet ground state He₂CCSD(T)/av5z reference calculation. An important property of the CCSD(T) method is its size-consistency which makes the above counterpoise correction possible. The ICMRCI method, on the other hand, is usually not enough size-consistent even with the Davidson correction applied. In this study we rely on the approximate way of performing the BSSE correction for the ICMRCI calculations. The third term in Eq. (1) is calculated via FCI for the ground state He atom. The second term is more difficult to handle and much of the error originates from this term. We calculate the corresponding excited excimer state in the basis of the supermolecule and approximate the third term of Eq. (1) with the energy obtained from this calculation. Here the active space consisted of the orbitals belonging to the He₂^{*} excimer. Finally, it should be noted that the present ICMRCI calculations are reaching close to the FCI level, and as such, a near size-consistency is expected.

The interatomic distances, R_{X-He} , measured from the center of mass of He₂^{*}, were systematically explored between 2.5 and 20 bohr (at least 16 points for each curve). All the (U/R)CCSD(T) and internally contracted MRCI calculations were carried out with the MOLPRO2000.1 program.²³

III. RESULTS AND DISCUSSION

A. He₂^{*}

The calculated diatomic states for He₂^{*} as obtained from the ICMRCI calculation are shown in Fig. 1. The ³a and ³c states calculated with the CCSD(T)/av5z method follow closely these curves. Overall agreement with the known experimental data and expectations provided in Ref. 4, is quite good. Table I lists the relevant data at the He₂^{*} equilibrium bond length by using various methods. All states, except one, can be identified according to the available experimental data and previous calculations. The fifth root in A₁ symmetry (labeled as ³?) does not fit to any experimental observation.²⁴

TABLE I. Atomic and diatomic excitation energies. The atomic energies are expressed relative to He(¹S) and diatomic energies are relative to ground state He₂(¹Σ_g) with $R = 1.05$ Å. Energies are expressed in eV and transition moments in Debye. Basis set is denoted as 1 = AV5Z, 2 = Ref. 21, and 3 = AV6Z. † in the R_e column indicates that the calculation was performed at this bond length only. Experimental transition moments are based on selection rules.

State	Configuration	Asymptote	Energy	R_e	Method	Transition moments
¹ S	<i>chgc</i> col;xin1s ²	...	0.0
³ S	1s2s	...	19.87	...	FCI/1	...
³ S	1s2s	...	19.77	...	FCI/2	...
³ S	1s2s	...	19.86	...	FCI/3	...
³ S	1s2s	...	19.82	...	Expt.	...
³ P	1s2p	...	22.54	...	FCI/1	...
³ P	1s2p	...	20.94	...	FCI/2	...
³ P	1s2p	...	22.25	...	FCI/3	...
³ P	1s2p	...	20.96	...	Expt.	...
³ S	1s3s	...	22.67	...	FCI/2	...
³ S	1s3s	...	22.72	...	Expt.	...
³ P	1s3p	...	23.01	...	FCI/2	...
³ S	1s3p	...	23.01	...	Expt.	...
<i>a</i> ³ Σ _u	1σ ² 1σ*2σ	1s2s	0.0	1.05†	CCSD(T)/1	...
<i>a</i> ³ Σ _u	1σ ² 1σ*2σ	1s2s	0.00	1.05†	MRCI/1	...
<i>a</i> ³ Σ _u	1σ ² 1σ*2σ	1s2s	0.00	1.05†	CCSD(T)/2	...
<i>a</i> ³ Σ _u	1σ ² 1σ*2σ	1s2s	0.00	1.05	MRCI/2	<i>b</i> (13.4), <i>c</i> (7.6), <i>e</i> (10.4),?(0.1)
<i>a</i>³Σ_u	1σ²1σ*2σ	1s2s	0.00	1.04	Expt.	<i>b,c,e,?</i>
<i>b</i> ³ Π _g	1σ ² 1σ*1π	1s2p _{x,y}	1.82	1.05†	CCSD(T)/1	...
<i>b</i> ³ Π _g	1σ ² 1σ*1π	1s2p _{x,y}	1.80	1.05†	MRCI/1	...
<i>b</i> ³ Π _g	1σ ² 1σ*1π	1s2p _{x,y}	0.64	1.05†	CCSD(T)/2	...
<i>b</i> ³ Π _g	1σ ² 1σ*1π	1s2p _{x,y}	0.62	1.05†	MRCI/2	<i>a</i> (13.4), <i>d</i> (4.4), <i>f</i> (6.4), <i>f</i> (4.8)
<i>b</i>³Π_g	1σ²1σ*1π	1s2p_{x,y}	0.59	1.06	Expt.	<i>a,d,f,f</i>
<i>c</i> ³ Σ _g	1σ ² 1σ*2σ*	1s2s	1.51	1.05†	CCSD(T)/1	...
<i>c</i> ³ Σ _g	1σ ² 1σ*2σ*	1s2s	1.50	1.05†	MRCI/1	...
<i>c</i> ³ Σ _g	1σ ² 1σ*2σ*	1s2s	1.38	1.05†	CCSD(T)/2	...
<i>c</i> ³ Σ _g	1σ ² 1σ*2σ*	1s2s	1.35	1.10	MRCI/2	<i>a</i> (7.6), <i>d</i> (6.4), <i>f</i> (8.5), <i>f</i> (15.0)
<i>c</i>³Σ_g	1σ²1σ*2σ*	1s2s	1.35	1.10	Expt.	<i>a,d,f,f</i>
<i>d</i> ³ Σ _u	1σ ² 1σ*3σ	1s2p _z	2.54	1.08	MRCI/2	<i>b</i> (4.4), <i>c</i> (6.4), <i>e</i> (31.2),?(16.8)
<i>d</i>³Σ_u	1σ²1σ*3σ	1s2p_z	2.53	1.07	Expt.	<i>b,c,e,?</i>
<i>e</i> ³ Π _g	1σ ² 1σ*2π	1s3p _{x,y}	2.72	1.08	MRCI/2	<i>a</i> (10.4), <i>d</i> (31.2), <i>f</i> (12.2), <i>f</i> (10.3)
<i>e</i>³Π_g	1σ²1σ*2π	1s3p_{x,y}	2.67	1.07	Expt.	<i>a,d,f,f</i>
<i>f</i> ³ Σ _u	1σ ² 1σ*4σ	1s3s	2.69	1.09	MRCI/2	<i>b</i> (6.4), <i>c</i> (8.5), <i>e</i> (12.2),?(9.4)
<i>f</i>³Σ_u	1σ²1σ*4σ	1s3s	2.67	1.08	Expt.	<i>b,c,e,?</i>
<i>f</i> ³ Π _u	1σ ² 1σ*1π*	1s2p _{x,y}	2.69	1.09	MRCI/2	<i>b</i> (4.8), <i>c</i> (15.0), <i>e</i> (10.3),?(18.0)
<i>f</i>³Π_u	1σ²1σ*1π*	1s2p_{x,y}	2.70	1.08	Expt.	<i>b,c,e,?</i>
? ³ Σ _g	1σ ² 1σ*3σ*	1s2p _z	2.92	1.08	MRCI/2	<i>a</i> (0.1), <i>d</i> (16.8), <i>f</i> (9.4), <i>f</i> (18.0)
?³Σ_g	1σ²1σ*3σ*	1s2p_z	Expt.	<i>a,d,f,f</i>

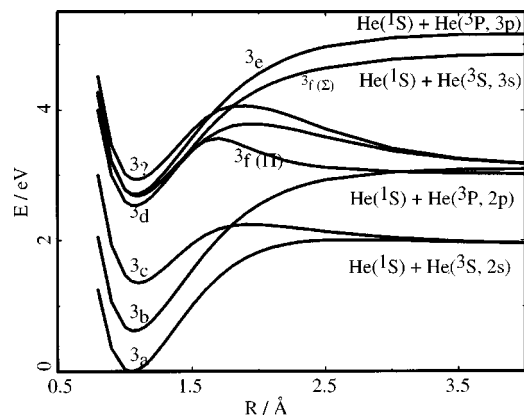


FIG. 1. Potential energy curves for eight lowest triplet states for He₂^{*} as obtained from ICMRCI calculations with basis set of Ref. 21. Asymptotic limits have not been adjusted.

This state was obtained as a side product in avoiding a root-flipping problem in the ICMRCI calculation and will not be further considered. The calculated transition dipole moments are in good agreement with expectations based on selection rules for homonuclear diatomics. Energetics and equilibrium bond lengths can also be considered to match the experimental observations well. Differences between the calculated and experimental transition energies are on the order of 10 meV.

Contour plots of the Rydberg electron natural orbitals are presented in Fig. 2. In the ^{3a} state the Rydberg electron is predominantly in the bonding combination of He 2s atomic orbitals; and the wave function exhibits near spherical symmetry at long distances from the ionic core. In contrast, in the ^{3c} state, the Rydberg electron is in the corresponding antibonding combination of the atomic 2s-orbitals as evidenced by the nodal plane between the two nuclei. For higher states, as the asymptote corresponding to the 2p atomic level is reached, the shape of the Rydberg orbital becomes less predictable. For example, in the ^{3d} state, the constructive combination of two 2p_z orbitals produces a rather diffuse spherical Rydberg electron with a radial node, as illustrated in the electron density plot of Fig. 3. These features will have important consequences with regard to the solvation shell in the liquid phase. In essence a bubble state describes a solvation shell that is effectively repelled by the electron, one in which the liquid avoids wetting the electron. In the case of very diffuse electron wave functions that contain nodes, we may expect the He solvent to penetrate the electron density, and therefore lead to partial wetting of the Rydberg electron. In such considerations, it is also important to discern the extent to which the electron density may be perturbed by the liquid. To this end, we will consider the ^{3d} state more closely, including the inspection of the electronic structure in the He₂^{*}-He complex. With regard to the diatomic Rydberg states, the electronic wave functions of the triplets are very similar to those of their singlet counterparts, and all discussions given therein are applicable to the present.⁵

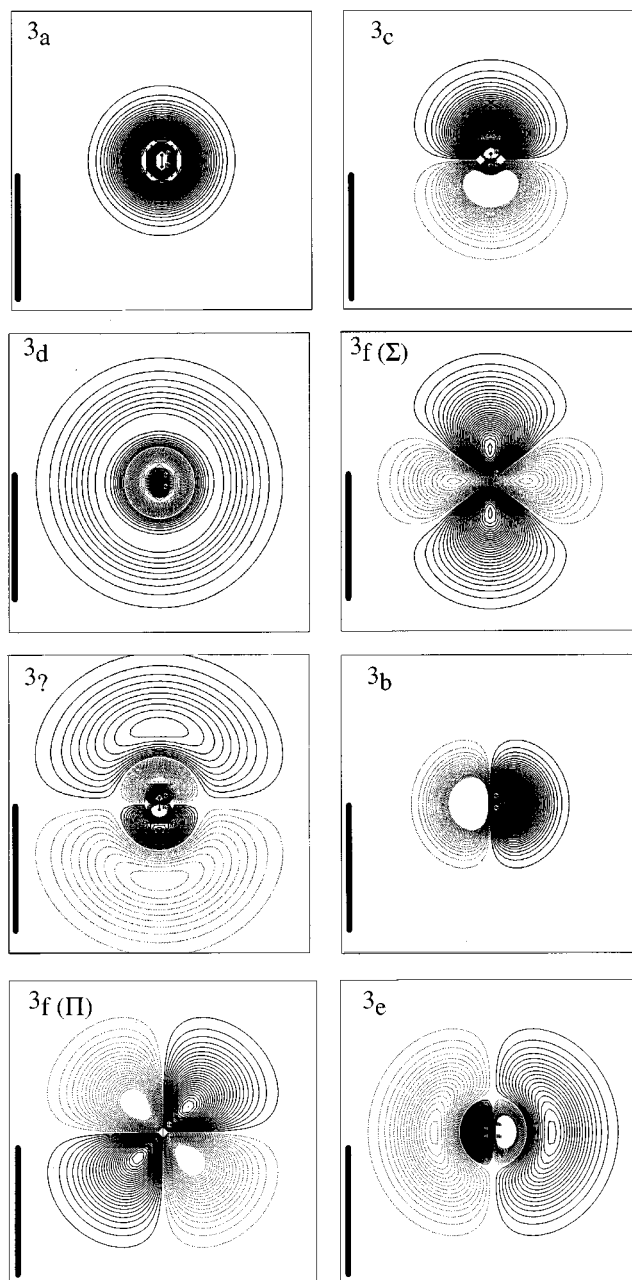


FIG. 2. Natural Rydberg orbital plots of He₂^{*} as obtained from ICMRCI calculations with the basis set of Ref. 21. The scale for the figures is set by the He₂^{*} center, with $R_e = 1.05$ Å. For clarity of the scale, we provide the solid line of length 10 Å in each to the left of each density plot. The contour level step is 0.001.

B. He₂^{*}-He

Selected tri- and tetra-atomic He₂^{*}(^{3a} and ^{3c})-He_n (where $n = 1, 2$) systems were computed with both CCSD(T) and ICMRCI methods with av5z basis, av6z basis, and the basis set of Ref. 21. In the ^{3a} state, at the potential minimum, the calculated energy difference between av5z and av6z bases is less than 0.1 cm⁻¹, while on the repulsive wall, the largest difference is ≈ 10 cm⁻¹ at $R = 3.5$ Å (2% difference). In the ^{3c} state, which contains a deep potential well of ~ 400 cm⁻¹, the variation in energy obtained by using the two different bases is less than 1 cm⁻¹. We may conclude that at the av6z level, the CCSD(T) calculations are converged with

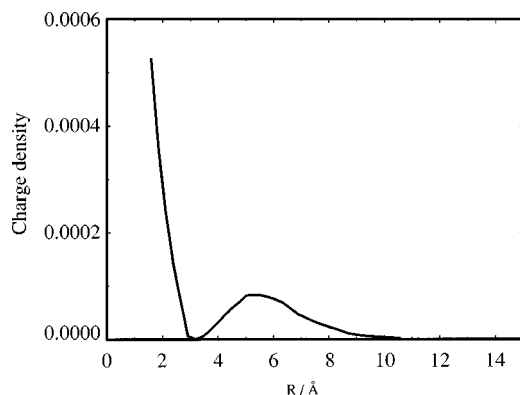


FIG. 3. Total electronic charge density of the 3d state excimer as a function of distance.

respect to the basis set. The average difference between ICMRCI and CCSD(T) at the av5z level was $\approx 1 \text{ cm}^{-1}$ at the potential minimum, the difference reflecting the degree of success of the BSSE correction in the ICMRCI calculation. Comparing the av5z results with the basis set of Ref. 21, at the CCSD(T) level, produced an average difference of 2 cm^{-1} at the potential minimum. This difference is attributed

to the missing high angular momentum Gaussians in the basis set of Ref. 21, bases which are required to describe electron correlation to the full extent. Since the bubble structure is a sensitive function of the long-range part of the interaction potential, we apply CCSD(T)/av6z to describe the 3a and 3c states whereas we apply the ICMRCI with the basis set of Ref. 21 to all other states.

Because the Pauli repulsion is expected to dominate long-range interactions, the He_2^*-He potential can be expected to follow the excimer electron density distribution rather closely. The diatomic Rydberg electron wave functions, as shown in Fig. 2, therefore provide qualitative expectations for the triatomic He_2^*-He interaction potentials. Thus, while the interaction potential for the 3a state must be isotropic, and the 3c state is strongly angle dependent. The triatomic energies, obtained from CCSD(T) and ICMRCI calculations, are given in Table II. Both collinear (L) and broadside (T) approach of the ground state He atom are considered in the case of anisotropic electronic wave functions. Selected potentials are shown graphically in Fig. 4. Let us highlight some of the salient features of these potentials:

(i) The 3a state is nearly isotropic at long distance. The anisotropy of the core only becomes evident on the repulsive

TABLE II. Computed potential energies for selected He_2^*-He interactions based on CCSD(T)/av6z for 3a and 3c states (using tetra-atomic configuration, with energy scaling to triatomic), and ICMRCI/Ref. 21 for all other states. The state labels refer to the electronic state of the excimer. The units are in cm^{-1} and Å. For the anisotropic potentials cuts along “ L ”-linear and “ T ”-shaped geometries are reported. In the $^3\Pi$ state, * indicates that the π orbital of the excimer is in the triatomic plane.

R	$a^3\Sigma_u L$	$a^3\Sigma_u T$	$c^3\Sigma_g L$	$c^3\Sigma_g T$	$d^3\Sigma_u L$	$d^3\Sigma_u T$	$e^3\Sigma_g L$	$e^3\Sigma_g T^*$	$e^3\Pi_g T$	$f^3\Sigma_u L$	$f^3\Sigma_u$
1.5	2477
1.75	345.6	272.6	549.5	27.9	778.4	245.4	409.2	67.7
2.0	-452.6	-693.2	-9.3	-572.2	256.2	-161.1	-153.2	-425
2.25	-482.0	-698.9	-285.7	-547.1	62.9	-263.6	70.1	-552
2.5	-394.2	-560.6	-354.8	-401.3	40.8	-236.2	431.4	-494
2.75	-300.3	-429.9	-319.4	-273.6	69.8	-184.8	741.0	-386
3.0	-206.4	-319.0	-250.0	-181.7	108.4	-141.3	991.6	-275
3.5	493.1	453.4	...	-100.9	-149.3	-110.2	-84.4	208.1	-88.1	1347.2	-94.6
4.0	256.0	210.6	...	-48.5	-31.4	-12.0	-42.8	339.6	-59.3	1435.5	3.1
4.5	109.2	91.2	766.0	-22.9	44.5	45.4	-25.1	450.3	-42.1	1157.8	40.0
5.0	43.2	37.2	411.9	-10.7	88.6	77.4	-16.0	513.4	-30.0	875.5	56.4
5.5	16.0	14.1	214.4	-5.1	107.5	90.8	-10.9	524.9	-21.4	648.6	63.0
6.0	5.2	4.8	107.1	-2.5	108.8	91.6	-7.8	487.8	-15.1	470.7	64.3
6.5	1.2	1.4	50.7	-1.3	98.9	83.8	-5.6	411.8	-10.5	334.7	62.6
7.0	-0.1	0.2	22.2	-0.8	82.8	71.1	-4.0	318.6	-7.3	233.7	58.9
7.5	-0.3	-0.2	9.0	-0.5	65.0	56.5	-3.0	230.2	-5.0	160.5	53.2
8.0	-0.3	-0.2	3.3	-0.3	48.3	42.6	-2.0	159.0	-3.4	108.6	45.8
8.5	-0.2	-0.1	1.8	-0.2	34.4	30.5	-1.4	107.3	-2.3	72.3	36.7
9.0	-0.1	-0.1	0.2	-0.1	23.6	21.0	-1.0	71.5	-1.5	47.4	27.4
9.5	0.0	-0.1	0.0	0.0	15.6	13.9	-0.8	47.5	-1.0	30.7	19.1
10.0	0.0	0.0	0.0	0.0	10.0	8.9	-0.6	31.3	-0.7	19.6	12.5
10.5	0.0	0.0	0.0	0.0	6.2	5.5	-0.4	20.4	-0.5	12.3	7.9
11.0	0.0	0.0	0.0	0.0	3.7	3.3	-0.3	13.2	-0.3	7.6	4.8
11.5	0.0	0.0	0.0	0.0	2.2	1.9	-0.2	8.4	-0.2	4.7	2.8
12.0	0.0	0.0	0.0	0.0	1.2	1.0	-0.1	5.3	-0.1	2.8	1.5
12.5	0.0	0.0	0.0	0.0	0.6	0.5	-0.1	3.2	-0.1	1.7	0.8
13.0	0.0	0.0	0.0	0.0	0.3	0.2	-0.1	2.0	-0.1	1.0	0.4
13.5	0.0	0.0	0.0	0.0	0.1	0.1	-0.1	1.2	-0.1	0.5	0.2
14.0	0.0	0.0	0.0	0.0	0.0	0.0	0.0	0.7	0.0	0.3	0.1
14.5	0.0	0.0	0.0	0.0	0.0	0.0	0.0	0.3	0.0	0.1	0.0
15.0	0.0	0.0	0.0	0.0	0.0	0.0	0.0	0.2	0.0	0.1	0.0
15.5	0.0	0.0	0.0	0.0	0.0	0.0	0.0	0.1	0.0	0.0	0.0
16.0	0.0	0.0	0.0	0.0	0.0	0.0	0.0	0.0	0.0	0.0	0.0

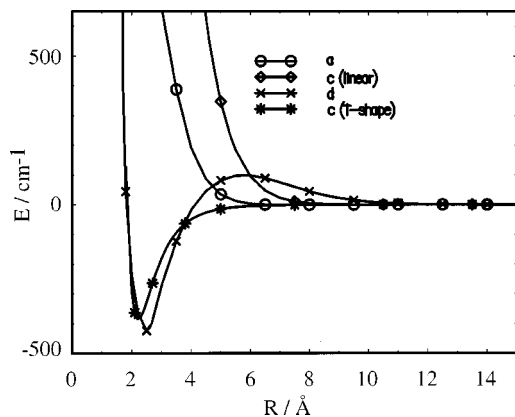


FIG. 4. He₂^{*}–He potentials for linear ³*a*, linear ³*c*, T-shaped ³*c*, and spherically averaged ³*d* states as obtained from ICMRCI/Ref. 21 calculations.

wall of the potential. It can be verified in Table II that at $R = 3.5 \text{ \AA}$ on the repulsive wall, the collinear approach produces a potential which is $\sim 8\%$ more repulsive than in the “*T*”-approach. Although the interaction is essentially repulsive throughout, both “*L*”- and “*T*”-geometries contain very shallow van der Waals minima of -0.3 cm^{-1} and -0.2 cm^{-1} near 8 \AA , respectively. Given the small magnitude of the anisotropy of the potential (0.1 cm^{-1} at the minimum) and the large rotational constant of He₂^{*} ($B = 7.7 \text{ cm}^{-1}$),²⁴ we may expect the ³*a* excimer to undergo free rotation in the liquid phase. This is consistent with the experimental observation of rotational structure in the $b \leftarrow a$ absorption spectrum in LHe.⁶ In short, ³*a* state can be expected to exist in a classic, spherical bubble in liquid He.

(ii) In the ³*c* state, while the potential in the collinear geometry is strictly repulsive, the “*T*”-approach leads to a deep minimum of 482 cm^{-1} at $R = 2.25 \text{ \AA}$ (see Table I). Despite this very deep binding, we have verified that this configuration is stable in the geometry-unrestricted sense. By using the restricted energy minimum of the He₂^{*}(³*c*)–He complex as an initial guess, unrestricted geometry optimizations within C_{2v} symmetry fail to produce a new minimum. At the minimum energy configuration, the Hessian obtained by the finite difference method was positive definite, indicating that a tightly bound He₃^{*} does not form spontaneously via the ³*c* state. Along the He₂^{*}–He stretching coordinate, the “*T*” complex can sustain four bound vibrational states. However, as can be recognized from the electron density plot in Fig. 2, this corresponds to motion in the nodal trough with very steep potential walls along the bending coordinate. Inclusion of the zero-point energy of bending greatly reduces the number of bound states in the complex (see the closely related system of He-molecular halogen complexes²⁵). In the liquid phase, the collective interaction with the bulk leads to defining the He density around the excimer. Now zero-point contributions to surface tension will dictate the extent of localization of He-density in the angularly sharp potential minimum on the nodal plane. A distorted bubble geometry with He localized at the belt of the excimer (analogous to some ²*P* state atoms in LHe) (Ref. 26) is to be expected.

(iii) The interaction potential in the ³*d* state is nearly isotropic at $R > 6 \text{ \AA}$, but becomes increasingly anisotropic at

shorter distances (see Table II). The potential contains a barrier of $\sim 100 \text{ cm}^{-1}$ at 6 \AA , followed by a deep minimum of $\approx 700 \text{ cm}^{-1}$ at 2.25 \AA along the collinear approach, 355 cm^{-1} along the “*T*”-approach. These features directly track the electron density in the He₂^{*}(³*d*) state, which is shown in Fig. 3. The potential energy barrier corresponds to the maximum of the Rydberg electron density in the outermost lobe, and the potential energy minimum occurs at the radial node. For binding to occur, the ground state He atom must penetrate the diffuse outer density of the Rydberg electron, by overcoming the barrier. Accordingly, both structure and dynamics of this state in the liquid phase can be expected to depend on the method of preparation. Once the liquid is expelled, at a bath temperature of $T \leq 2.14 \text{ K}$, the barrier of 140 K could in principle keep the deep potential well dry. With the same consideration, if He density were to reach the well, it could in principle freeze out of the bath. A more detailed analysis of the bubble structure is deferred.⁹

(iv) In the $e \text{ } ^3\Pi_g$ state, the collinear approach leads to an attractive potential, while the “*T*” approach breaks the degeneracy of the state into: an attractive potential for the Π -orbital perpendicular to the plane of the triatomic, and a repulsive potential for the coplanar configuration. The coupling of the electron orientation with the nuclear coordinate will lead to Jahn–Teller activity, with asymmetric bubble motions required to break the electronic degeneracy of the Π state.

(v) In higher Rydberg states, the obvious trends of angular and radial nodes seen in the electron density plots of Fig. 2 will be reflected in the interaction potentials. As a representative of these states, we consider the ³*f* state, which can be seen in strong-field preparations.² We give potential energy points along the *L*- and *T*-approach of He₂^{*}(³*f*)–He in Table II.

Quite clearly, in proceeding from potential energy curves of triatomics to energetics of solvation in the liquid phase, many-body effects need to be assessed. We have explored such effects explicitly, by calculating the energetics of tetra-atomics at the same level of theory as the triatomics, and testing the additivity of the weak interaction. The studies were limited to the ³*a*, ³*c*, and ³*d* states. For linear and T-shaped ³*a* and linear ³*c* many-body effects are very small ($< 0.2 \text{ cm}^{-1}$). However, for the T-shaped ³*c*, which contains a deep minimum of $\sim 400 \text{ cm}^{-1}$ at close range (see Fig. 4), nonadditivity effects are noticeable. When two ground state He atoms approach the He₂^{*}(³*c*) state along the perpendicular bisector of the excimer (“cross”-geometry), the minimum energy configuration occurs at a distance 0.2 \AA longer than in the triatomic “*T*”-complex. Since the potential minimum in this case is predominantly due to induction, this short-range nonadditivity effect can be rationalized in terms of polarization. Polarization effects can be expected to be further amplified in the liquid phase. The same short-range effect is operative at the potential minimum in the ³*d* state. Additionally, a very different source of nonadditivity can be identified at long-range, in the diffuse region of the Rydberg electron density. This is illustrated in Fig. 5. In Fig. 5(a) we plot both the tri- and tetra-atomic He₂^{*}–He potentials (scaled to triatomic case). The potential minimum of the tetra-atomic

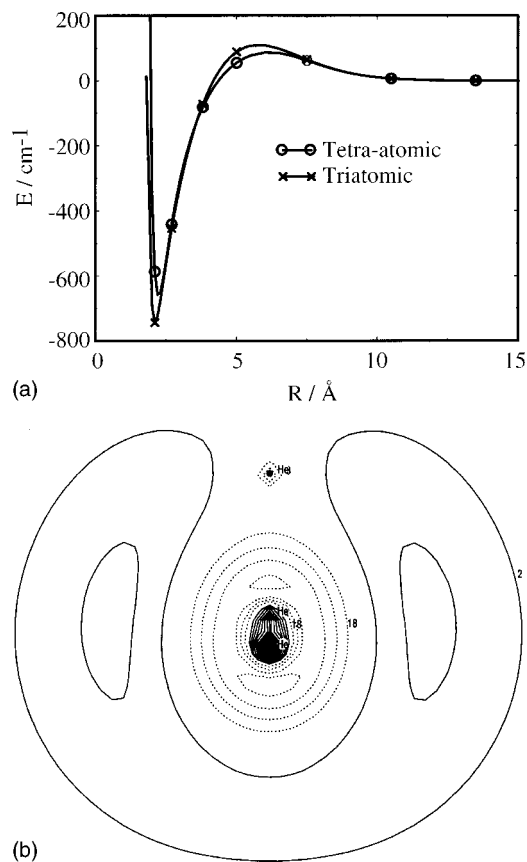


FIG. 5. Nonadditivity of interactions: (a) Comparison of potentials for linear $\text{He}_2^*(^3d)\text{-He}$ as obtained from calculation of the triatomic and tetra-atomic complex (scaled to triatomic) using ICMRCI/Ref. 16. (b) Effect of a single ground state He atom on the Rydberg electron wave function (natural orbitals) of $\text{He}_2^*(^3d)$ at the ICMRCI/Ref. 16 level. One contour level corresponds to 0.005.

is shifted by $\approx 0.2 \text{ \AA}$ to longer distances along with a small reduction in binding energy. Deviations from additivity can also be seen at the potential barrier, starting at a distance near 7.2 \AA . The origin of this non-additivity is visualized in Fig. 5(b), where it can be seen that the approaching ground state He atom effectively repels the diffuse Rydberg electron density. In effect, the ground state atom parts the electron density as it approaches the excimer. Note that this effect is distinct from the nonadditivity of induction forces, which must also be taken into account in any polarizable medium. In the tetra-atomic, the presence of another ground state He atom at the same radial separation (opposite side) increases the angular confinement of the electron, hence the higher barrier. Accordingly, significant modification of the barrier region is to be expected in the liquid phase. As example, along the symmetric breathing coordinate of the bubble, complete angular confinement of the Rydberg electron must generate a much larger barrier than in the case of the triatomic. At distances longer than 7 \AA ($E < 50 \text{ cm}^{-1}$), many-body effects appear to be negligible.

The electron-helium pseudopotential has been commonly used in descriptions of atomic and molecular excited centers in liquid helium.^{27,28} It is then valuable to compare the present *ab initio* potentials to what would be obtained by the pseudopotential method. In this approach the effective

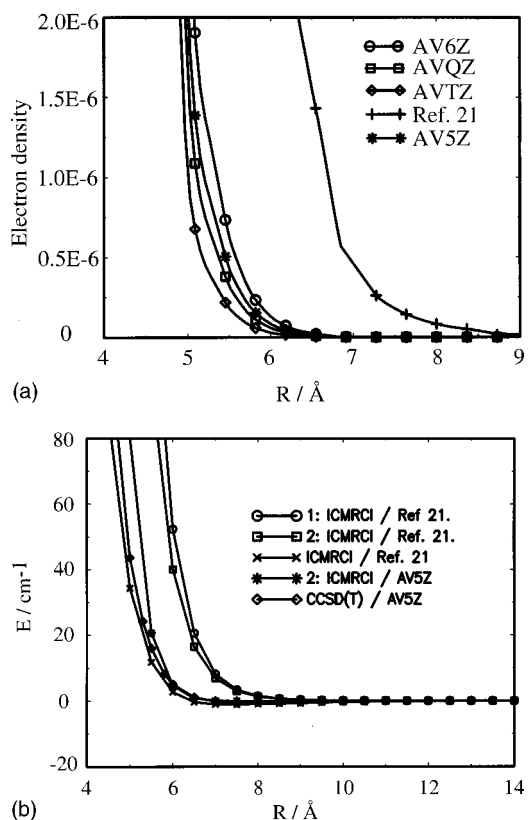


FIG. 6. Electron densities and pseudopotentials: (a) Convergence of the $\text{He}_2^*(^3a)$ electron density with the basis set. (b) Comparison between pseudopotential approach [Eq. (2) of text], and strictly *ab initio* calculations of the triatomic $\text{He}_2^*(^3a)\text{-He}(^1S)$ potential. Scheme 1 denotes $A = 49.76 \text{ meV}$ and $\beta = 2.6 \text{ \AA}^{-1}$, whereas in 2, $A = 17.8 \text{ meV}$ and $\beta = 2.15 \text{ \AA}^{-1}$ (see Ref. 28).

interaction energy of the excimer with the ground state He atom, $\tilde{V}(r)$, is treated as a sum of repulsion and attraction,

$$\tilde{V}(r) = \int V_{\text{ps}}(|r-r'|)\rho(r')d^3r' - \frac{1}{2}\alpha|E(r)|^2, \quad (2a)$$

where

$$V_{\text{ps}}(r) = A \exp(-\beta r). \quad (2b)$$

The repulsive part of the effective potential is obtained by convoluting the total electron density of the excimer, $\rho(r)$, with the exponentially repulsive electron-helium pseudopotential, V_{ps} . While, the attractive contribution is obtained by first calculating the electrostatic potential, $E(r)$, by integrating over the charge distribution of the excimer and then evaluating the energy of a polarizable He atom in the resultant electric field. The total electron density from ICMRCI calculations, and electron-helium interaction parameters from Ref. 27, were used in the evaluation of Eq. (2). In all cases the attractive term was negligible at distances larger than 5 \AA , therefore, the potential shape is almost exclusively determined by the pseudopotential integral. This integral is very sensitive to the electron density at large distances from the excimer and therefore sensitive to the basis set used. This effect is illustrated in Fig. 6(a), where the electron density is shown in the region of the onset of repulsion. Figure 6(b) shows the calculated potentials as obtained from the pseudo-

potential approach as well as the *ab initio* calculation. Although there is a significant variation in the electron densities from one basis set to another, the variation in calculated *ab initio* energies is much smaller. Since the pseudopotential method reflects the electron density, it generates large differences in effective potentials derived from the different basis sets. The comparison suggests that the basis set of Ref. 21 produces a small amount of spurious electron density at long distances from the excimer, but it appears that this density is easily removed by an approaching ground state He atom (in triatomic configuration). The pseudopotential calculation using ICMRCI/av5z total electron density produces reasonably accurate results at long distances when compared to the corresponding CCSD(T)/av5z calculation (error < 0.6 cm⁻¹ for $R > 6.0 \text{ \AA}$). At short distances the pseudopotential method produces considerably more repulsive potentials than the *ab initio* calculations. The difference between pseudopotentials calculated with av5z and av6z at $R = 6.5 \text{ \AA}$ is $\approx 0.4 \text{ cm}^{-1}$. This small difference suggests that the av6z basis set would not produce significantly more repulsion in He₂^{*}-He, another indication that with respect to the basis set, convergence has been reached.

As a calibration of the accuracy of the CCSD(T)/av5z calculations a comparison was made against the He-Li system, where the pair potential is known with good accuracy.²⁹ The CCSD(T)/av5z method produces a slightly more repulsive pair potential, with a difference of 0.6 cm⁻¹ at the potential minimum ($R_e = 6 \text{ \AA}$). Since this calculation involves one less electron than He₂^{*}-He, the comparison can be expected to yield a lower limit for the error in He₂^{*}-He potential in ³*a* and ³*c* states. We estimate the accuracy of the derived *ab initio* potentials to be between 0.6 cm⁻¹ and 2 cm⁻¹ in the region of the potential minima. Another closely related system that was used as a test case is the H₂-He system. Spectra of both singlet and triplet H₂ in liquid He have been obtained recently, and have been analyzed to conclude that H₂ occurs in a bubble state, with a bubble radius of 8.1 Å for the H₂(³*a*).³⁰ The CCSD(T)/av5z level of theory, with the BSSE correction, produces a spherical potential which extends slightly to longer distances than the ³*a* state of He₂^{*}. By calculating the effective bubble potential according to the model used in Ref. 30, but using the H₂(³*a*)-He potential obtained from the CCSD(T)/av5z treatment we obtain a very similar bubble potential. In our calculation, the bubble energy was minimized at $\approx R_b = 7.5 \text{ \AA}$. The difference of 0.6 Å between the value we calculate, and the radius obtained in Ref. 30 is representative of the uncertainty to be expected in calculations strictly based on *ab initio* potentials.

IV. CONCLUSIONS

We have presented potential energy curves that provide a good description of the He₂^{*}-He interaction, with the excimer in its various triplet states. The error in the pair potentials for ³*a* and ³*c* states, at the potential minimum region, is estimated to be less than 2 cm⁻¹ and somewhat higher for the other states which were obtained from ICMRCI calculations. The accurate description of these potentials is invaluable

to understanding the solvation of these excited centers in superfluid helium^{3,9} and their spectroscopy.³¹

ACKNOWLEDGMENTS

This research is supported through grants from the U.S. National Science Foundation (9725462), the U.S. Air Force Office of Scientific Research (F49620-98-1-0163), and through a Fellowship provided to one of the authors (J.E.) by the Science Academy of Finland.

- ¹N. Schwentner E.-E. Koch, and J. Jortner, *Springer Tracts in Modern Physics: Electronic Excitations in Condensed Rare Gases* (Springer-Verlag, New York, 1985), Vol. 107.
- ²A. Benderskii, R. Zadoyan, and V. A. Apkarian, *J. Chem. Phys.* **110**, 1542 (1999).
- ³A. Benderskii, J. Eloranta, R. Zadoyan, and V. A. Apkarian (in preparation); preliminary reports of this work have appeared: A. V. Benderskii, R. Zadoyan, N. Schwentner, V. A. Apkarian, *SPIE* **3273**, 297 (1998); V. A. Apkarian, A. Benderskii, and J. Eloranta, *Am. Chem. Soc.* **220**, 136-Phys. Part 2 (2000).
- ⁴M. L. Ginter and R. Battino, *J. Chem. Phys.* **52**, 4469 (1970).
- ⁵S. L. Guberman and W. A. Goddard, *Phys. Rev. A* **12**, 1203 (1975).
- ⁶J. C. Hill, O. Heybey, and G. K. Walters, *Phys. Rev. Lett.* **26**, 1213 (1971).
- ⁷W. S. Dennis, E. Durbin, W. A. Fitzsimmons, O. Heybey, and G. K. Walters, *Phys. Rev. Lett.* **23**, 1083 (1969); J. W. Keto, F. J. Soley, M. Stockton, and W. A. Fitzsimmons, *Phys. Rev. A* **10**, 887 (1974).
- ⁸A. P. Hickman and N. F. Lane, *Phys. Rev. Lett.* **26**, 1216 (1971); J. P. Hansen and E. L. Pollock, *Phys. Rev. A* **5**, 2214 (1972).
- ⁹J. Eloranta and V. A. Apkarian (in preparation).
- ¹⁰K. Raghavachari, G. W. Trucks, J. A. Pople, and M. Head-Gordon, *Chem. Phys. Lett.* **157**, 479 (1989); P. J. Knowles, C. Hampel, and H.-J. Werner, *J. Chem. Phys.* **99**, 5219 (1993); C. Hampel, K. Peterson, and H.-J. Werner, *Chem. Phys. Lett.* **190**, 1 (1992); Perturbative triples correction program by M. J. O. Deegan and P. J. Knowles, 1992.
- ¹¹C. Janssen and H. F. Schaefer III, *Theor. Chim. Acta* **79**, 1 (1991).
- ¹²T. J. Lee and P. R. Taylor, *Int. J. Quantum Chem.* **23**, 4936 (1989).
- ¹³R. M. Jordan, H. R. Siddiqui, and P. E. Siska, *J. Chem. Phys.* **84**, 6719 (1986).
- ¹⁴A. R. Janzen and R. A. Aziz, *J. Chem. Phys.* **107**, 914 (1997).
- ¹⁵S. M. Cybulski and R. R. Toczyowski, *J. Chem. Phys.* **111**, 10520 (1999).
- ¹⁶H.-J. Werner and P. J. Knowles, *J. Chem. Phys.* **89**, 5803 (1988); P. J. Knowles and H.-J. Werner, *Chem. Phys. Lett.* **145**, 514 (1988); *Theor. Chim. Acta* **84**, 95 (1992).
- ¹⁷P. J. Knowles and H.-J. Werner, *Chem. Phys. Lett.* **115**, 259 (1985); H.-J. Werner and P. J. Knowles, *J. Chem. Phys.* **82**, 5053 (1985).
- ¹⁸M. R. A. Blomberg and P. E. M. Siegbahn, *J. Chem. Phys.* **78**, 5682 (1983); S. R. Langhoff and E. R. Davidson, *Int. J. Quantum Chem.* **8**, 61 (1974).
- ¹⁹G. Schaftenaar and J. H. Noordik, *J. Comput.-Aided Mol. Design* **14**, 123 (2000).
- ²⁰D. E. Woon and T. H. Dunning, Jr., *J. Chem. Phys.* **100**, 2975 (1994). For description of av6z, see Extensible Computational Chemistry Environment Basis Set Database as developed and distributed by the Molecular Science Computing Facility, Environmental and Molecular Sciences Laboratory which is part of the Pacific Northwest Laboratory, P.O. Box 999, Richland, WA 99352.
- ²¹K. K. Sunil, J. Lin, H. Siddiqui, P. E. Siska, K. D. Jordan, and R. Shepard, *J. Chem. Phys.* **78**, 6190 (1983); C. F. Chabalowski, J. O. Jensen, D. R. Yarkony, and B. H. Lengsfeld III, *ibid.* **90**, 2504 (1989).
- ²²F. Boys and F. Bernardi, *Mol. Phys.* **19**, 553 (1970).
- ²³MOLPRO is a package of *ab initio* programs written by H.-J. Werner and P. J. Knowles, with contributions from R. D. Amos, A. Bernhardsson, A. Berning *et al.*, *Theor. Chim. Acta* **85**, 423 (1993); F. Eckert, P. Pulay, and H.-J. Werner, *J. Comput. Chem.* **18**, 1473 (1997).
- ²⁴G. Herzberg, *Molecular Spectra and Molecular Structure I. Spectra of Diatomic Molecules*, 2nd ed. (Krieger, Malabar, 1989).
- ²⁵J. Williams, A. Rohrbacher, J. Seong, N. Marianagam, K. C. Janda, R. Burcl, M. M. Szczesniak, G. Chalasiński, S. M. Cybulski, and

- N. Halberstadt, *J. Chem. Phys.* **111**, 997 (1999); M. I. Hernandez, N. Halberstadt, W. D. Sands, and K. C. Janda, *ibid.* **113**, 7252 (2000).
- ²⁶J. Reho, U. Merker, M. R. Radcliff, K. K. Lehmann, and G. Scoles, *J. Chem. Phys.* **112**, 8409 (2000).
- ²⁷J. Jortner, N. R. Kestner, S. A. Rice, and M. H. Cohen, *J. Chem. Phys.* **43**, 2614 (1965); K. Hirioke, N. R. Kestner, S. A. Rice, and J. Jortner, *ibid.* **43**, 2625 (1965).
- ²⁸B. Space, D. F. Coker, Z. H. Liu, B. J. Berne, and G. Martyna, *J. Chem. Phys.* **97**, 2002 (1992).
- ²⁹S. H. Patil, *J. Chem. Phys.* **94**, 8089 (1991).
- ³⁰A. Trottier, A. I. Jirasek, H. F. Tiedje, and R. L. Brooks, *Phys. Rev. A* **61**, 052504 (2000).
- ³¹J. P. Toennies and A. F. Vilesov, *Annu. Rev. Phys. Chem.* **49**, 1 (1998).